

# Application of birefringent filters for Thomson scattering

**J. Howard**

Plasma Research Laboratory,  
Australian National University  
Canberra ACT 0200

E-mail: [john.howard@anu.edu.au](mailto:john.howard@anu.edu.au)

**Abstract.** We propose wide field-of-view, high transparency birefringent filters (essentially fixed delay polarization interferometers) for incoherent Thomson scattering measurements of the temperature and density of plasma free electrons. A single filter, combined with imaging optics and dual detector arrays observing both dark and bright interference fringes, can give an unambiguous electron temperature estimate, even for blue shifted high temperature spectra. For multi-pulse systems, a switchable delay plate synchronized with the laser repetition rate can allow density and temperature to be obtained using a single detector array. This both simplifies relative channel calibration issues and opens the possibility for 2-D temperature imaging. We describe the measurement principle and present results of numerical simulations for low and high temperature scenarios. The approach is well suited to very high electron temperature measurement systems such as the lidar scheme proposed for the ITER tokamak.

## 1. Introduction

Laser Thomson scattering from free plasma electrons [1] is now the standard technique for measuring electron temperature in almost all terrestrial plasmas, from low temperature atmospheric arcs, through to magnetic fusion devices. Because of their small mass, the electrons can have velocities that are a substantial fraction of the speed of light. As a result the light scattered from an illuminating high-power pulsed laser source has high spectral bandwidth (low coherence). The scattered spectrum is usually measured using a low-resolution high-throughput grating spectrometer. By equipping the spectrometer with a 2-d intensified and gated CCD camera, it is possible to image the entire laser stripe in the plasma and so obtain spatially resolved electron temperature and density information, albeit at a relatively low repetition rate. [2].

A common approach to obtaining time resolved scattered spectra in multi-pulse laser systems is to use filter polychromators combined with an array of photomultiplier tube or avalanche photodiode detectors. By carefully calibrating

the filters it is possible to use the measured intensity ratios to estimate the spectral width and hence the electron temperature. Though imaging filter polychromators and detector arrays have been used successfully [3, 4], more often, each spatial channel uses a dedicated polychromator with a photo-detector for each spectral bin. For high spatial resolution systems, this presents a formidable problem in terms of expense, maintenance and calibration.

We propose a method based on measurement of the optical coherence of the scattered radiation at a fixed optical delay. High throughput, wide field-of-view polarization interferometers have been used recently for Doppler imaging of ion temperature in the H-1 heliac [5, 6, 7]. The so-called MOSS (modulated optical solid-state) spectrometer monitors the complex coherence (fringe visibility and phase) of an isolated spectral line at one or more optical delays. When observing ion motions, the spectral width is small compared to the the light wavelength, necessitating the use of high spectral resolution (large delay) optical interferometers. In this article, we focus on the utility of birefringent plate interferometers for relatively low resolution spectral applications such as Thomson scattering.

In its simplest form, the collected scattered light is transmitted by a wide passband pre-filter to a polarization interferometer that uses a final Wollaston prism to form distinct images of the antiphase components of the optical coherence (bright and dark fringes) onto parallel detector arrays. The difference between the bright and dark fringes normalized to the mean bears a simple monotonic relationship to the electron temperature, while the mean of the two signals normalized to the pulse energy is proportional to the electron density. Because of the simple relationship between fringe contrast and electron temperature, two dimensional temperature imaging becomes feasible using either a high power expanded laser beam, or by using mirrors to translate the multiply-reflected laser beam across the plasma region of interest. As we show below, the interferometric optical delay is chosen so as to optimally utilize all of the photons transmitted by the pre-filter.

For repetitive-pulse scattering systems, and using a suitably modulated dual-delay system synchronized with the laser pulse rate, it is possible to combine signals from alternate pulses to obtain the electron density and temperature using a single detector element. This has the advantage of simplifying relative channel sensitivity calibration. Alternatively, such systems could be configured to extend the dynamic range of the temperature measurement by using multiple switchable delays.

This paper is organized as follows. In section 2 we briefly review the relationship between the Thomson scattered spectrum and its optical coherence. We then describe a birefringent filter suitable for simultaneously monitoring orthogonally polarized output images of light scattered from a probing laser beam. The filter response, including material dispersive properties, is modeled for both low and high temperature cases. We also present a time-multiplex variant of the

split-image system suitable for use in repetitive-pulse systems. This approach has the advantage of requiring only a single detector element per spatial channel. In section 3 we discuss experimental considerations as they apply to the use of birefringent filters, namely stray and plasma light issues, and suggest a means for calibration of the system response in the difficult, high-temperature, wide passband case.

## 2. Measurement principle

The birefringent filter (polarization interferometer) is composed of a birefringent plate sandwiched between polarizers. Radiation that traverses the first polarizer is incident on a birefringent plate whose fast axis is oriented at  $45^\circ$  to the polarization direction. The plate splits the incident scattered scalar wave component  $u(t)$ , relatively delaying nominally equal amplitude components by time  $\tau$  before they are recombined at a final polarizer and focused onto a square-law detector. The intensity of the transmitted or reflected light is proportional to

$$S_{\pm}(\tau) = \frac{I_0}{2} \left[ 1 \pm \Re[\tilde{\gamma}(\tau)] \right] \quad (1)$$

where  $I_0 = \langle u u^* \rangle$  is the spectrally integrated irradiance, or brightness, and  $\tilde{\gamma}$  is the complex coherence given by  $\tilde{\gamma} = \langle u(t) u^*(t + \tau) \rangle / I_0$  where angle brackets denote a time average [8]. In general, the complex temporal coherence is related to the spectral distribution of the irradiance  $I(\nu)$  through the Wiener-Khinchine theorem

$$\tilde{\gamma}(\tau) = \frac{1}{I_0} \int_{-\infty}^{\infty} I(\nu) \exp(i2\pi\nu\tau) d\nu. \quad (2)$$

For relatively narrowband spectra, the interferometric phase delay can be approximated by

$$\begin{aligned} \phi &= 2\pi\nu\tau(\nu) \\ &\approx \phi_0 + \kappa\phi_0\xi \end{aligned} \quad (3)$$

where we have substituted  $\nu = \nu_0(1 + \xi)$  where  $\xi = (\nu - \nu_0)/\nu_0$  is a normalized frequency difference coordinate,  $\phi_0 = 2\pi\nu_0\tau_0$  where  $\tau_0$  is the centre-frequency time delay and where

$$\kappa = 1 + \frac{\nu_0}{\tau_0} \frac{\partial\tau}{\partial\nu} \Big|_{\nu_0} \quad (4)$$

accounts for any optical frequency dispersion of the time delay. Using (3) in equations (1) and (2) obtains the interferogram

$$S_{\pm}(\phi_0) = \frac{I_0}{2} \left[ 1 \pm \Re[\tilde{\gamma}(\hat{\phi}_0) \exp(i\phi_0)] \right] \quad (5)$$

where the self coherence is given by

$$\tilde{\gamma} = \frac{1}{I_0} \int_{-\infty}^{\infty} I(\xi) \exp(i\hat{\phi}\xi) d\xi \quad (6)$$

and it is convenient to introduce the group phase delay

$$\hat{\phi}_0 = \kappa\phi_0. \quad (7)$$

For a given scattering geometry, and assuming the electrons to be in thermal equilibrium, the shape of the incoherent Thomson spectrum can be generally expressed in terms of the electron temperature alone. Accurate analytic approximations to the form of the spectrum valid for relativistic energies have been reported [9]. The scattered spectrum gives information about the velocity distribution function in the direction  $\mathbf{k} = \mathbf{k}_s - \mathbf{k}_i$ , where  $\mathbf{k}_s$  and  $\mathbf{k}_i$  are wavevectors for the scattered and incident beams respectively [10]. For low electron temperatures (less than a few hundred eV), the spectral dependence of the scattered radiation is well approximated by

$$I_T(\xi; T_e) = I_0(\pi\xi_{\text{th}}^2)^{-1/2} \exp(-\xi^2/\xi_{\text{th}}^2) \quad (8)$$

with

$$\xi_{\text{th}} \equiv 2 \sin(\theta/2) v_{\text{th}} \quad (9)$$

and where  $\theta$  is the angle between the incident and scattered wavevectors,  $T_e$  is the electron temperature and  $v_{\text{th}}$  is the electron thermal speed normalized to the speed of light. Because the spectrum is a function of only a single parameter, measurement of the coherence at a single fixed delay offset  $\phi_0$  is sufficient to obtain  $T_e$ .

The simple birefringent filter shown schematically in figure 1, uses interference techniques to estimate the optical coherence length. The normal-incidence time delay introduced by a birefringent crystal plate of thickness  $L$  and birefringence  $B$  is  $\tau_0 = LB/c$ . For radiation of centre frequency  $\nu_0$ , the interferometer signal at either of the final polarizer ports is given by

$$S_{\pm} = \frac{I_0}{2}(1 \pm \zeta \cos \phi_0) \quad (10)$$

where  $I_0$  is the brightness of Thomson scattered light transmitted by the first polarizing beamsplitter,  $\phi_0 = 2\pi\nu_0\tau_0 = 2\pi N$  is the monochromatic birefringent phase delay and  $N$  is the order of interference. The fringe visibility (fringe amplitude normalized to mean intensity)  $\zeta = \zeta_I\zeta_T$  includes an instrumental component  $\zeta_I$  due to the average of the birefringent plate delay over the angular extent of the source (analogous to the familiar slit function for grating spectrometers) as well as the degradation  $\zeta_T$  due to the finite source spectral width. The instrument function is determined via a suitable calibration procedure as discussed in section 3.

For a low temperature thermal distribution, the fringe visibility associated with the Thomson scattered light takes the simple form

$$\zeta_T(\phi_0) = \exp[-\hat{\phi}_0^2 \sin^2(\theta/2)v_{\text{th}}^2] = \exp(-T_e/T_C) \quad (11)$$

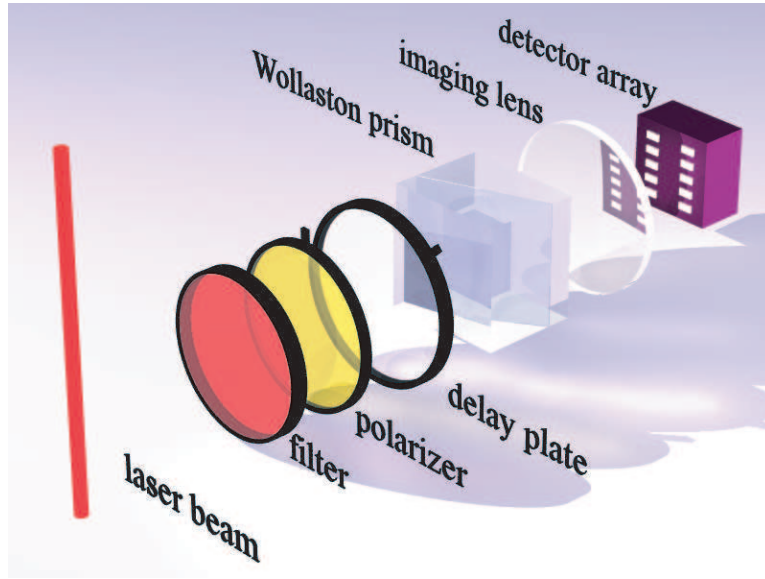


**Figure 1.** Layout for simple coherence imaging filter for Thomson scattering. The final Wollaston polarizer produces separate images of the bright and dark fringes onto the detector array. For optical systems that preserve the polarization of the scattered radiation, the first polarizer can be superfluous.

where  $T_C$  is a “characteristic temperature” set by the waveplate delay and the scattering angle:

$$kT_C = \frac{1}{2}m_e c^2 / [\hat{\phi}_0 \sin(\theta/2)]^2. \quad (12)$$

Optimum sensitivity to temperature variations is obtained when the optical delay is chosen such that  $T_e \sim T_C$ , or  $\Delta\nu/\nu_0 \sim 1/N$  where  $\Delta\nu/\nu_0$  is the Thomson spectral bandwidth [6].

Thomson spectra and their associated interferograms for temperatures in the range 100-500 eV for a birefringent filter based on a quartz waveplate are shown in figure 2. The interferogram calculations take into account the wavelength-dependence of the quartz birefringence and assume that the full spectrum is observed. It can be seen that the variation of fringe visibility with temperature is best measured by setting  $\phi_0/2\pi = M/2$  where  $M$  represents an integer number of half waves. At this delay, the scattered signals are

$$S_{\pm} = \frac{I_0}{2}[1 \pm \zeta_T] \quad (13)$$

where  $\zeta_T(\phi_0)$  is the Thomson spectrum fringe contrast at delay  $\phi_0 = M\pi$ . The signals derived from both the orthogonally polarized light components produced by the final Wollaston polarizer, are sufficient to determine the total scattered power and the contrast degradation due to the Doppler broadening:

$$\zeta_T = \frac{S_+ - S_-}{S_+ + S_-}. \quad (14)$$

The effects of possible stray light contamination are considered below.

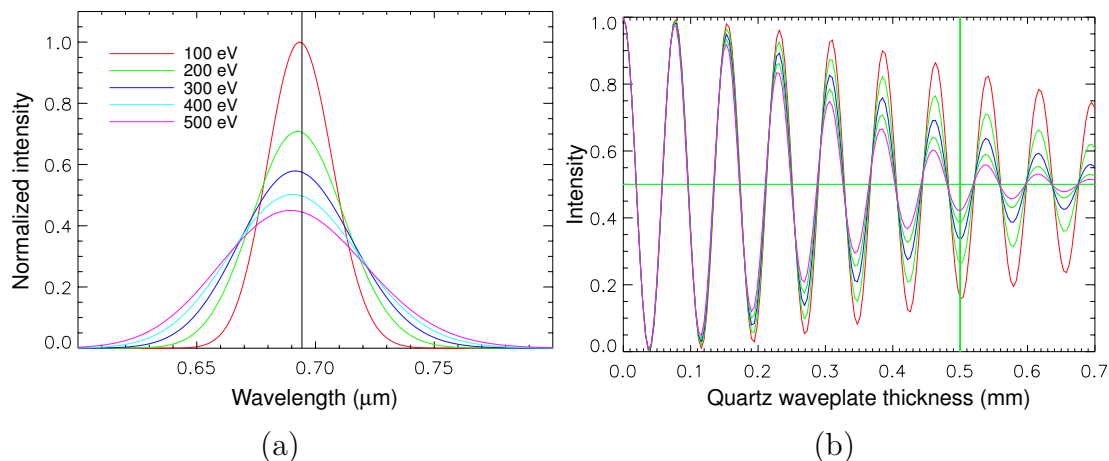


**Figure 2.** (a) Thomson scattered spectra for temperatures in the range 100–500 eV. We have assumed  $90^\circ$  viewing geometry and a ruby laser source (694.3 nm). (b) The calculated interferograms. A quartz waveplate of thickness 0.5 mm is optimum for sensing temperature variations near 200 eV.

As a concrete example, for an electron temperature  $T_e = 200$  eV, and  $90^\circ$  scattering, the condition  $T_e = T_C$  requires  $N = 6.45$  waves delay at the ruby laser wavelength 694.3 nm.  $M = 13$  half waves can be obtained using a crystal quartz birefringent plate of thickness  $L = 0.50$  mm ( $n_{E0} = 1.550$ ,  $n_O = 1.541$ ,  $\kappa = 1.24$ ). Because the required quartz plate is thin, sensitivity to ambient temperature changes can be ignored.

### 2.1. High temperature case

When the temperature exceeds 1keV, the Thomson spectrum broadens and shifts to the blue. However, it is the shift of the spectrum that most sensitively conveys the temperature, and this is registered by the interferogram as a phase change. To illustrate this, we model a YAG-laser based ( $1.06 \mu\text{m}$ )  $90^\circ$  scattering system. For simplicity, we assume a flat spectral response for the detector and other optical components, and calculate the interferogram for ideal transmission colour filters spanning 650–1050 nm (figure 3) and 450–1050 nm (figure 4) respectively.

Compared with the narrowband interferograms shown in figure 3(b), the wideband interferograms [figure 4(a)] have much smaller coherence length, and, as expected, show a dispersion of interferometric phase with temperature. In each case, one monitors the interferogram at a waveplate thickness selected to deliver a sensitive variation of the interferogram amplitude with electron temperature. The dependence of fringe amplitude on electron temperature for both the narrow and broadband cases at waveplate thicknesses 0.115 and 0.055 mm respectively, are shown in figure 4(b). It is evident that the wideband measurements are more responsive to higher temperature variations. However, the use of such large passbands also admits disproportionately more plasma continuum and line radiation background. This light will contribute to the interferogram, and must

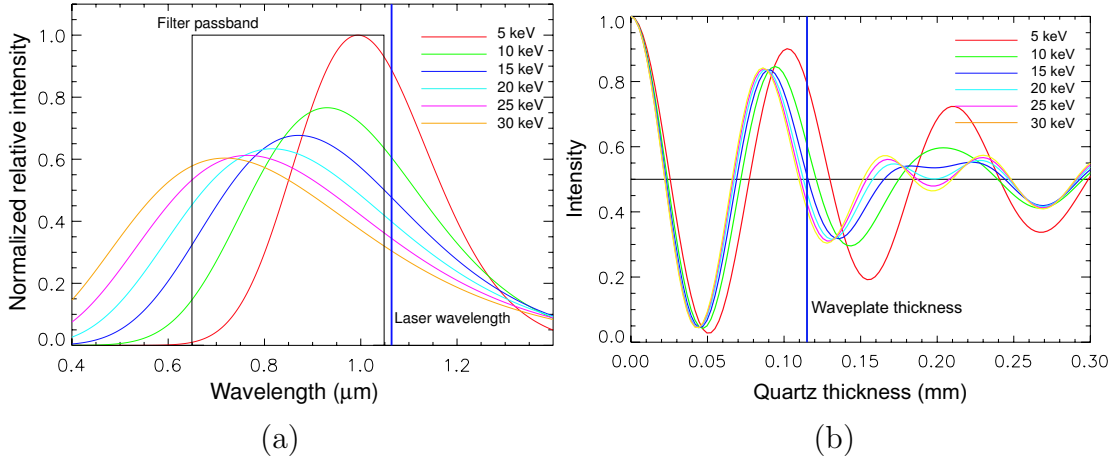


**Figure 3.** (a) The Thomson spectra in the range 5 to 30 keV for 1.06  $\mu\text{m}$  excitation and ninety degrees observation angle. (b) The associated interferograms using a quartz-based polarization interferometer and for a top-hat colour filter centred on 850nm with 400nm bandpass. The vertical line indicates the selected quartz waveplate thickness of 0.115mm.

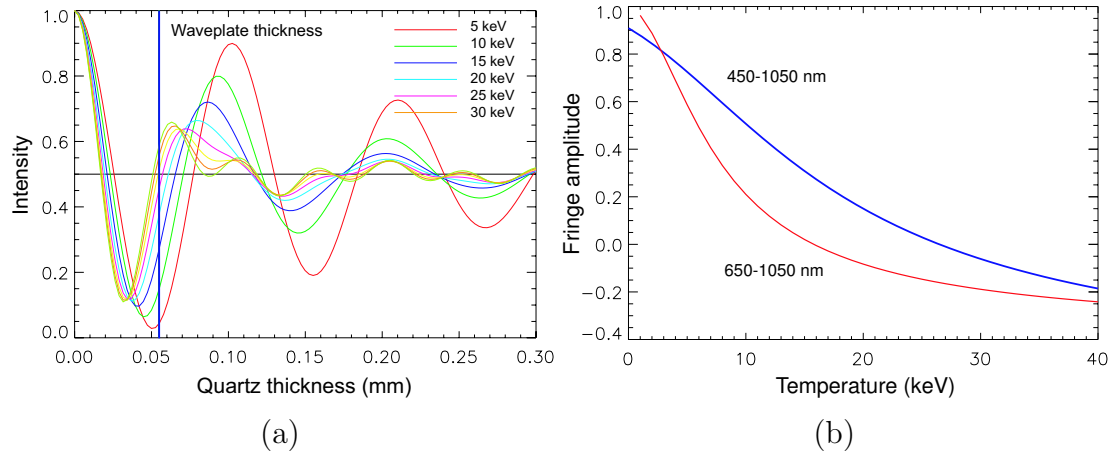


**Figure 4.** (a) The interferograms calculated for a quartz-based polarization interferometer and for a top-hat filter spanning 450nm to 1050nm. The vertical line indicates the selected quartz waveplate thickness of 0.055mm. (b) Variation of normalized fringe amplitude with temperature for the narrow (400 nm) and wide (600 nm) passband filters. and for quartz waveplate thicknesses of 0.115mm and 0.055mm respectively. Sensitivity to high temperature variations increases with colour filter bandwidth. See text for discussion.

be measured separately from the Thomson pulse. To alleviate this problem, it may be desirable to observe the more compact Thomson spectrum obtained by collecting the scattered radiation at smaller angles to the probing beam.

The effects of birefringence dispersion become more significant for broadband measurements [see (4)]. For example both lithium tantalate  $\text{LiTaO}_3$  and magnesium fluoride  $\text{MgF}_2$  have low birefringence in the visible region. However, in contrast with  $\text{MgF}_2$ , the optical transmission for  $\text{LiTaO}_3$  deteriorates below 450nm and the birefringence dispersion increases [figure 6(a)]. As shown in figure

5, the stronger birefringence dispersion for LiTaO<sub>3</sub> increases the variation of interferogram phase shift with temperature, but is countered by an associated decrease in fringe visibility. The result is that the overall variation of normalized fringe amplitude with temperature at high temperatures is comparable for both waveplates [figure 6(b)] and no advantage is obtained. However, the enhanced dispersion with plate thickness evident for LiTaO<sub>3</sub> suggests that, for more detailed spectral studies of the Thomson spectrum, a wedged birefringent plate between polarizers, combined with a 2-d detection system might offer a high-throughput time-domain alternative to imaging grating-based CCD systems.

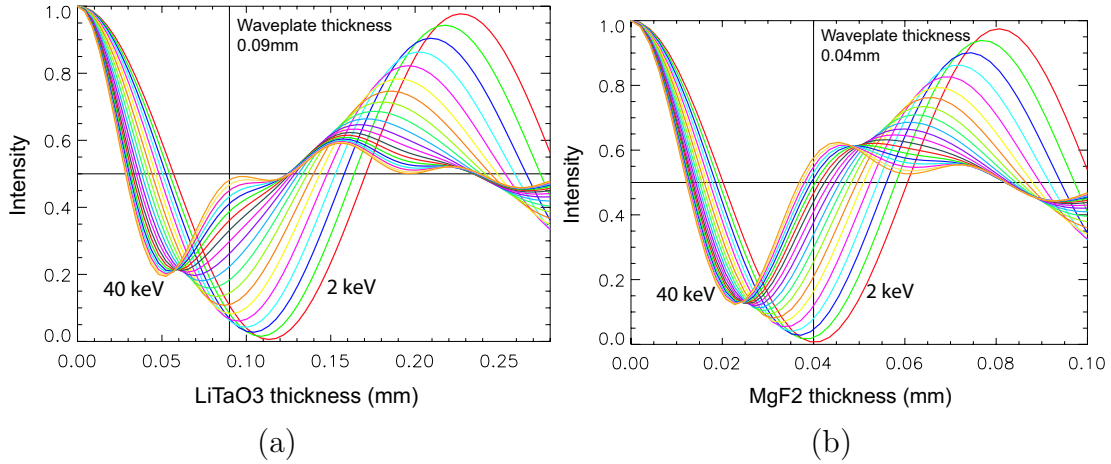


**Figure 5.** The Thomson interferograms in the range 2, (2), 40 keV for 1.06  $\mu\text{m}$  excitation, filter passband 400-1000nm and ninety degrees observation angle. (a) Dispersive LiTaO<sub>3</sub> waveplate and (b) MgF<sub>2</sub> waveplate. The vertical lines in each case indicate the selected contrast thicknesses for computation of the temperature-dependent fringe contrast.

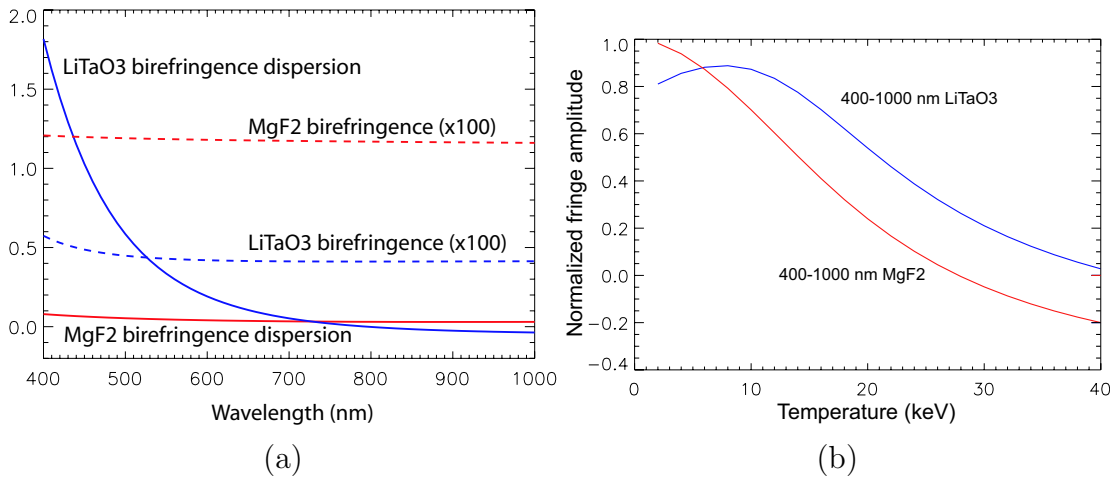


**Figure 6.** (a) Birefringence  $B = n_e - n_o$  and birefringence dispersion  $|(\lambda/B)(dB/d\lambda)|$  for MgF<sub>2</sub> and LiTaO<sub>3</sub> waveplates in the range 400-1000nm and (b) the variation of fringe contrast with electron temperature for ideal wide-band (400-1000nm) filter and both MgF<sub>2</sub> and LiTaO<sub>3</sub> waveplates. See text for discussion.

## 2.2. Modulated single-detector systems

For multi-pulse Thomson systems, a temporal multiplex approach can be used to obtain a true single-detector estimate of the electron temperature. A fast (1kHz) switching ferro-electric liquid crystal (FLC) placed between parallel polarizers, and synchronized with the laser pulse rate, can alternately switch the optical delay between zero and some fixed offset delay provided by the FLC itself. With the FLC open (fast axis parallel with polarizers, zero nett delay), the transmitted signal is  $S_+ = I_0$  where  $I_0$  is the total scattered intensity. With the FLC switched (fast axis  $45^\circ$  to polarizers), the signal is  $S_+ = I_0(1 + \zeta_T)/2$ , where  $\zeta_T$  is the normalized fringe amplitude at the inserted delay. The two measurements are sufficient to allow the determination of the electron temperature and density provided that these quantities do not vary significantly on the timescale of the period between laser pulses. One can also envisage the use of multiple switched FLC cells that allow probing of the optical coherence at more than a single delay.

## 3. Experimental considerations

The interferogram depends on both the nature of the scattered spectrum  $I(\nu)$  as well as the overall system spectral response  $R(\nu)$  which includes the collection and processing optics and detection system. In this case we can recast (2) as

$$\zeta = \Re(\tilde{\gamma}) = \frac{1}{I_0} \int_0^\infty R(\nu) I(\nu) d\nu. \quad (15)$$

One means to determine the unknown response function  $R(\nu)$  could be to measure the variation of the normalized fringe amplitude  $\zeta^{\text{BB}} = \Re(\tilde{\gamma}^{\text{BB}})$  for blackbody radiation as a function of the source temperature. For a given temperature  $T_j$ , (15) can be discretized in terms of the unknown spectral response coefficients  $R_i \equiv R(\nu_i)$  as:

$$\zeta^{\text{BB}}(T_j) = \sum_i I_{ji}^{\text{BB}} R_i \quad (16)$$

where  $I_{ji}^{\text{BB}}$  is the blackbody spectral irradiance at temperature  $T_j$  and optical frequency  $\nu_i$ . For a sufficient number of measurements, (16) can be inverted for the response vector  $\{R_i\}$ . We have not attempted to estimate the condition of this procedure. Nevertheless, simulations for the case shown in figure 4 show that substantial contrast variations are achievable for blackbody temperature variations in the range 500 to 3000K. An alternative calibration approach may be to measure the interferogram and thereby estimate the coefficients  $\{R_i\}$  using a light source of known spectrum and a set of optical bandpass filters. With the spectral response determined, the absolute sensitivity can be obtained using either the standard Rayleigh or Raman scattering techniques [11].

Because of the need for the first polarizing element, the maximum throughput is only 50%. However, because of the simplicity of the optical arrangement, it may be possible to install the polarization interferometer so as to

view directly the polarized scattered laser light. The final polarized coherence-images of the laser stripe can then be coupled to optical fibre bundles for transport to remote detection systems.

Because the delay is small, birefringent filters will generally have a wide field-of-view. Any off-axis or wide-field effects will be captured by the system calibration. Standard field-widening techniques [12] can be utilized in the case where the response is otherwise degraded by angular averaging over a range of phase delays.

As is usual, the level of stray laser light can be estimated by measuring the mean of the signals  $S_+$  and  $S_-$  in the absence of plasma. Plasma background light must also be monitored and subtracted from the measured signals  $S_{\pm}$ . The unknown plasma background interferogram can be measured in a time window displaced from the laser pulse and then subtracted from the overall signals.

#### 4. Conclusion

The optical systems proposed here offer some advantages over traditional polychromator systems for the analysis of Thomson scattering spectra. Birefringent filters can have high transparency, large aperture and a wide, uniform field-of-view. They are therefore ideal for 2-d time-resolved wide-band spectral imaging applications. The Thomson systems described here utilize a single filter and one or two detector arrays to obtain images of the electron temperature and density.

#### Acknowledgments

The author would like to thank Dr T. Hatae from JT-60U for useful discussions and for providing information relating to the nature of the high temperature Thomson spectrum.

#### References

- [1] J. Sheffield, *Plasma Scattering of Electromagnetic Radiation* (Academic Press, New York, 1975).
- [2] M. N. A. Beurskens, C. J. Barth, N. J. Lopes Cardozo, and H. J. Van der Meiden, *Plasma Phys. Control. Fusion* **41**, 1321 (1999).
- [3] D. Dimock *et al.*, *Rev. Sci. Instrum.* **68**, 700 (1997).
- [4] H. Yoshida *et al.*, *Rev. Sci. Instrum.* **70**, 747 (1999).
- [5] J. Howard, C. Michael, F. Glass, and A. Cheetham, *Rev. Sci. Instrum.* **72**, 888 (2001).
- [6] J. Howard, *Appl. Opt.* **41**, 197 (2002).
- [7] J. Howard, C. Michael, F. Glass, and A. Danielsson, *Plasma Phys. Control Fusion* **45**, 1143 (2003).
- [8] M. Born and E. Wolf, *Principles of Optics* (Pergamon Press, Oxford, 1980).
- [9] O. Naito, H. Yoshida, and T. Matoba, *Phys. Fluids B* **5**, 4256 (1993).
- [10] I. H. Hutchinson, *Principles of Plasma Diagnostics* (Cambridge University Press, Cambridge, 1987), p. 218.

- [11] J. Howard, B. James, and W. Smith, *J. Phys. D: Appl. Phys.* 1435 (1979).
- [12] W. Steel, *Interferometry* (Cambridge University Press, Cambridge, 1967).